

Electronic energy levels and carrier dynamics in InAs/InGaAs dots-in-a-well structure investigated by optical spectroscopy

Rui Chen,¹ H. Y. Liu,² and H. D. Sun^{1,a)}

¹*Division of Physics and Applied Physics, School of Physical and Mathematical Sciences, Nanyang Technological University, Singapore 637371, Singapore*

²*Department of Electronic and Electrical Engineering, University College London, Torrington Place, London WC1E 7JE, United Kingdom*

(Received 27 September 2009; accepted 26 November 2009; published online 7 January 2010)

We investigate the electronic energy levels and carrier dynamics in InAs/In_xGa_{1-x}As dots-in-a-well (DWELL) structure by comprehensive spectroscopic characterization over a temperature range from 10 to 300 K. The integrated photoluminescence (PL) intensity is observed to increase with raising temperature up to 100 K. Through combining the PL and PL excitation (PLE) analysis, we provide direct evidence that this anomalous temperature dependence of the PL spectrum is due to the carrier trapping in InGaAs quantum well at low temperature. A rate equation model is adopted to quantitatively describe the thermal escape and capture processes of carriers in the DWELL system. The origin of thermal activation energies for quantum dot PL quenching at higher temperatures is discussed referring to the electronic energy levels revealed by PLE spectra. © 2010 American Institute of Physics. [doi:10.1063/1.3277049]

I. INTRODUCTION

Indium arsenide (InAs), a small band gap (0.35 eV) semiconductor, is recognized as one of the most promising III-V group material. Considerable attention has been paid to InAs quantum dot (QD) materials due to their potential device applications in the wavelength range between 1.3 and 1.55 μm for optical fiber telecommunication. Long wavelength InAs QDs have been fabricated through atomic layer epitaxy, covering InAs QDs with InGaAs and/or AlAs cap layer, etc.¹ However, the shortcoming of those techniques lies in the low dot density which provides a low effective gain and is therefore more difficult to achieve lasing. Of the many techniques proposed and investigated, growing the dots within an InGaAs quantum well (QW), i.e., to form a so-called quantum dots-in-a-well (DWELL) structure, has been accepted as one of good approaches.² Indeed, high InAs QD density and good carrier capture ability have been demonstrated in this structure.³ To fabricate efficient laser device operating at room or even higher temperatures, a clear understanding of the effect of temperature on the optical properties is crucial. It is recognized that the temperature dependent optical properties of QD materials should be closely related to their electronic energy levels. For the relatively simple InAs/GaAs QD structure, a number of articles have been devoted to discuss the mechanisms of carrier capture and thermal quenching process but there is still no consensus.⁴⁻⁹ The issue becomes more complicated in DWELL structure, because a two-dimensional QW and a zero-dimensional QD are involved simultaneously. Up to now, the temperature dependent photoluminescence (PL) spectra of InAs/InGaAs DWELL structures and their fundamental properties are still under explanation, despite that the

DWELL structures have demonstrated promising potential in device application; especially existing discussion has not referred to the detailed electronic energy structures.¹⁰⁻¹⁶

In this paper, the electronic energy levels and carrier dynamics in an InAs/InGaAs DWELL structures are investigated by detailed PL and PL excitation (PLE) spectroscopy. We observed direct evidence that the unusual increase in integrated PL intensity with temperature should be attributed to carrier trapping in InGaAs QW. The temperature dependent PL data is quantitatively explained by a rate equation model referring to the electronic energy structures. The origin of thermal activation energies for QD PL quenching process at higher temperature is well elaborated. Our investigation provides significant insight into the mechanisms governing the optical properties of InAs/InGaAs DWELL structure, which is very important for optimal structure design and growth.

II. EXPERIMENTAL DETAILS

The samples used herein were grown in a VG Semicon V80H molecular beam epitaxy system on (100)-oriented GaAs substrates. QDs were formed by 2.9 ML InAs grown upon a 2 nm In_xGa_{1-x}As strained buffer layer, and then covered with a 6 nm In_xGa_{1-x}As strain-reducing layer. The indium composition x in InGaAs layers can be changed for tuning the wavelength. After the DWELL structure growth at 505 °C, the nanostructure was capped with 15 nm GaAs followed by a 120 s long growth interruption and further GaAs cap growth at 615 °C. The dot density of the structure was estimated to be around $3.1 \times 10^{10} \text{ cm}^{-2}$ from atomic force microscopy measurement. From our previous cross-sectional transmission electron microscopy and scanning tunneling microscopy studies, InAs QDs had a truncated pyramidal shape with typical size of 40–50 and 5–7 nm height. Detailed growth and characterization of this structure can be

^{a)}Author to whom correspondence should be addressed. Electronic mail: hdsun@ntu.edu.sg.

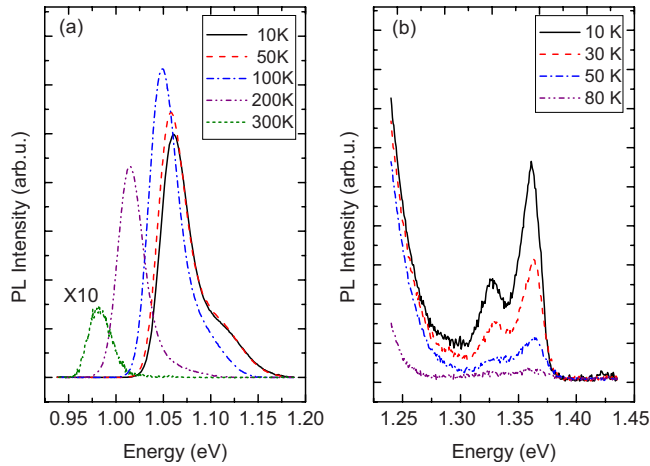


FIG. 1. (Color online) (a) Temperature dependent PL emission from InAs QDs and (b) from surrounding InGaAs QW.

found in the related references.^{17–19} The PL measurements were performed between 10 and 300 K within a closed-cycle helium cryostat. A cw He–Cd laser emitting at 442 nm was used for PL excitation source and the PL signal was dispersed by a 0.30 m grating monochromator and detected by a Peltier cooled InGaAs photodiode using standard lock-in amplifier technique. The PLE signal was detected using the same system at 10 K, except for the excitation source was replaced by a 250 W tungsten halogen lamp combined with a 0.27 m grating monochromator and suitable filters.^{20,21}

III. RESULTS AND DISCUSSIONS

Figure 1(a) shows the PL spectra of the sample (In composition $x=0.12$ in $\text{In}_x\text{Ga}_{1-x}\text{As}$ QW) at different temperatures. The excitation power density was controlled as low as 0.07 W cm^{-2} . At high temperature, the PL exhibits a single peak corresponding to the ground state (GS) emission in QDs. However, a nonsymmetrical PL line shape is observed at low temperature. The tail on the high energy side should not be attributed to an excited state (ES) emission since the PL spectra were measured at a low excitation regime far from the QD's GS saturation. Actually it is associated with GS emission from different sizes of QDs as a consequence of carriers' random distribution at low temperatures. The change in the PL line shape with temperature will be discussed later. The PL intensity is found to increase with increasing temperature up to 100 K. Similar behavior in InAs/InGaAs DWELL structure^{10,13,15} and CdTe QDs deposited on a wetting layer (WL) in a ZnTe matrix has been observed.²² In our investigation, we extended the measured wavelength range and a quite weak PL at higher energy (1.3–1.4 eV) is detected, as plotted in Fig. 1(b). Interestingly, the PL signal at higher energy decrease very quickly as temperature increases and totally disappears at temperature higher than 80 K. This new emission band has never reported before.

To clarify the origin of above PL features, we have performed detailed PLE measurement on the same sample, with mind that the PL properties should be related to the electronic structure of the material system. Figure 2 plots the PL and PLE spectra of the investigated sample taken at 10 K,

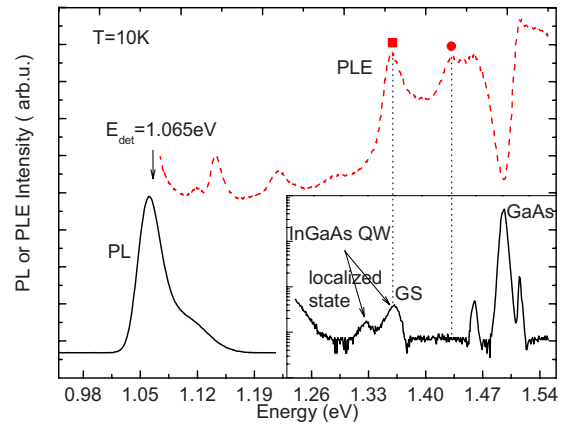


FIG. 2. (Color online) PL and PLE (dashed line) spectrum of the sample measurement at 10 K. The GS and ES of the bi-QW are marked by a closed square and closed circle, respectively. Inset is the PL from the InGaAs QW. Noticed that the y-ordinate use a logarithmic scale.

where the PLE was recorded at detection energy of 1.065 eV. The “resonantlike” peaks in the low energy region (1.10–1.30 eV) shift with the detection energy, which are related to longitudinal-optical (LO) phonon assisted carrier relaxation in QDs.^{23,24} The energy of the LO phonon estimated from PLE spectra is around 28.5 meV, which can be ascribed to InAs WL phonon.²⁵ Comparatively, the shape of the PLE spectra in higher energy region is independent of the detection energy. The features in this “nonresonant” excitation region are associated with the absorption of surrounding InGaAs QW and GaAs barrier. The PL features at energy higher than the QD emission shown in the inset of Fig. 2 should be assigned referring to the transition bands displayed in the PLE spectrum. The PL bands at 1.515, 1.497, and 1.461 eV are close to the exciton absorption peak. They apparently come from GaAs-related emission and are attributed to the recombination of free, donor-acceptor pairs and localized excitons, respectively.²⁶

Bearing in mind, a thin InAs WL will be formed before the three-dimensional growth of InAs QDs based on Stranski–Krastanov mode. This InAs WL together with the surrounding InGaAs QW composes a complex bi-QW between the dots. As shown in the PLE spectra of Fig. 2, the peak at 1.362 eV (marked by closed square) comes from the GS absorption in this bi-QW, while the peak at 1.434 eV (marked by closed circle) can be attributed to the optical absorption of higher ES, which is totally in agreement with our modeling by the eight-band $k \cdot P$ method. The simulated WL is 0.25 nm thick, which is in the physical realistic region.^{27,28} For comparison, measurement of samples with different In composition in the InGaAs QW is carried out. Figure 3 demonstrates the PLE spectra of those samples with different In composition in InGaAs QW. The schematic energy band diagram is shown in Fig. 3 where the solid lines and dashed lines denote the GS and ES of the bi-QW, respectively. As can be expected, the peaks related to GaAs remain unchanged while the GS (marked by closed squares) and ES (marked by closed circles) from the bi-QW shift with varying the In composition. The modeling results are listed in Table I. It is clearly seen that the simulated values fit the

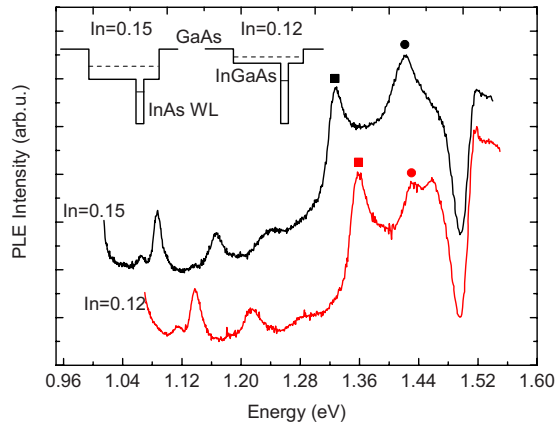


FIG. 3. (Color online) PLE spectrum of different In composition in InGaAs QW. Inset is the energy band diagram of the bi-QW concerning the InAs WL and the surrounding InGaAs QW. The GS and ES of the bi-QW are marked by closed squares and closed circles, respectively.

experimental data very well, which verifies the validity of our modeling and assignment. It is worthy of mentioning that the InGaAs bi-QW plays important role in the carrier relaxation processes. The bi-QW performs strong absorption and the captured carriers then can relax to the GS of the InAs QD with the participation of LO phonons. This is the reason why the InAs/InGaAs DWELL structure demonstrates more effective carrier capture ability compared with the traditional InAs/GaAs QD. Returning to the PL spectrum, the emission band at 1.362 eV can be assigned to the GS carrier recombination in the InGaAs bi-QW. The peak at 1.325 eV can be attributed to recombination of excitons localized at the interface between InAs QD and InGaAs QW.

The appearance of the QW-related emission provides strong evidence that there exists a barrier potential located at the QW interface, which could trap the carriers at low temperatures because otherwise the carriers excited should rapidly relax to the QDs. It is therefore deduced that after capping the 6 nm InGaAs layer, the strain field between InAs QDs and InGaAs QW creates a deformed energy profile at the interface, which forms a potential barrier and localized states. At low temperature, some of the carriers may be trapped by this potential barrier; therefore they recombine radiatively, giving the PL signal at higher energy [PL bands at 1.325 and 1.362 eV presented in Fig. 1(b)]. As the temperature increase, carriers trapped in the QW gain enough thermal energy to overcome this potential barrier and relax into the QD level resulting in the rapid decrease in QW-

TABLE I. Comparison of the simulated energies for the GS and the ES using eight-band $k \cdot P$ method with the experimentally measured values for two different DWELL samples.

In composition in $\text{In}_x\text{Ga}_{1-x}\text{As}$ QW	Experimental value (eV)		Simulated value (eV)	
	GS	ES	GS	ES
x=0.12	1.362	1.434	1.356	1.438
x=0.15	1.327	1.421	1.327	1.412

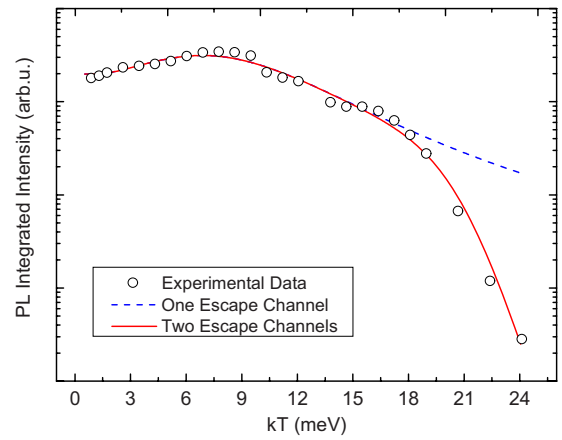


FIG. 4. (Color online) The integrated PL intensity of InAs/InGaAs DWELL structure as a function of temperature and the corresponding fit to one and two carrier escape channel from the Eq. (2).

related PL signal. Meanwhile, those thermalized carriers contribute to the increase in the QDs' PL intensity, as indicated in Fig. 1(a).

Figure 4 shows the integrated PL intensity of InAs/InGaAs DWELL structure with temperature change. Quantitatively, the temperature dependence of the PL intensity of QDs should be described by rate equation. From the model proposed by Popescu *et al.*,¹⁵ the integrated PL intensity in low temperature (10–100 K) can be expressed as

$$\frac{R_r N_D}{G_e} = \left[1 + \frac{K_0}{1 + \exp\left(-\frac{E_b}{kT}\right)} \right]^{-1}, \quad (1)$$

where R_r and N_D are the radiative recombination rate of excitons captured by QDs and the number of electrons in the QD, respectively. G_e is the number of carriers captured by the QW per unit time. K_0 is a constant, k is the Boltzmann constant, T is the temperature, and E_b denotes the potential barrier. For temperature higher than 100 K, thermal escape of carriers should be taken into account and the complete expression is given by the following equation:¹⁵

$$\frac{R_r N_D}{G_e} = \left\{ 1 + \frac{K_0}{1 + \exp\left(-\frac{E_b}{kT}\right)} \left[1 + \sum_i K_i \times \exp\left(-\frac{E_i}{kT}\right) \right] \right\}^{-1} \quad (i = 1 \text{ or } 2), \quad (2)$$

where i represents the number of channels for carriers thermal escape, K_i is a constant, and E_i is the thermal activation energy. Here the summation is over all the possible channels of carrier escape, which are related to the electronic structure of the material system.

By fitting the experimental data less than 100 K to Eq. (1), a value of 7.5 meV of the potential barrier E_b is obtained which is close to the value obtained by others.^{13,15} The amplitude of 7.5 meV trapping potential seems reasonable if taking into account the observation that the PL band near the QW absorption edge disappear at ~ 100 K (~ 8 meV). Next

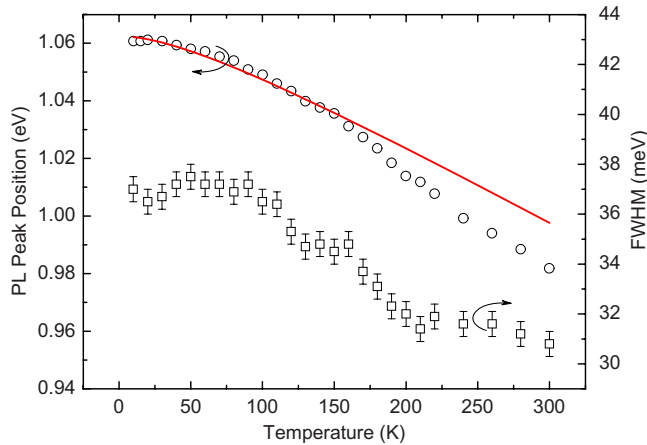


FIG. 5. (Color online) Temperature dependent PL peak position and FWHM of InAs QDs. Straight line is the InAs band gap shrinkage obtained from Varshni law.

we fit the temperature dependent integrated PL intensity in the whole measurement range using Eq. (2). If only a single thermal escape channel is considered, the model fits the experimental data well at temperature lower than 200 K. At higher temperature, however, significant deviation appears in the fitting, which implies that more thermal escape channels should be taken into account. We found that the temperature dependence of QD integrated PL intensity can be perfectly fitted by considering two escape channels. The carriers activation energies obtained are around 34 and 262 meV for E_1 and E_2 , respectively. The 34 meV activation energy is close to the thermally activated capture of excitations by nonradiative defects in GaAs.^{4,6,29} For nonresonant PL measurements, carriers are photogenerated in GaAs barrier and can undergo these extrinsic processes before they are captured by QDs. The 262 meV activation energy is close to the energy difference between the GS transition of QD and QW (~ 290 meV), indicating that it is due to the thermal escape of carriers from QD levels to InGaAs QW.

Figure 5 shows the temperature dependence of the PL peak position and full width at half maximum (FWHM). The InAs-like band gap shrinkage is also shown using the Varshni approximation.³⁰ The PL peaks match well with the tendency of InAs band gap up to 150 K. However, when further increasing temperature, the QD PL peak redshifts faster. As for FWHM, it keeps almost constant around 37 meV at low temperature. Then it exhibits a slow and monotonic decrease simultaneously with the faster redshift of the emission energies up to 200 K and remains constant at value about 31 meV for higher temperature, opposite to the trend of phonon broadening. These behaviors can be explained by the dynamic process between the thermalization and capture of carriers. At low temperatures, carriers are randomly frozen into the QD states and the PL is the superposition of emission arising from different size of QDs.³¹ At higher temperatures, carriers gain sufficient thermal energy and may be thermalized into the QW plane. As the barrier between the QW and QDs is not high, the carriers will be eventually recaptured by some other QDs. Apparently the higher the QD energy level (in small size QDs), the higher the probability is thermalized. On the other hand, the recaptured carriers

have more chance to relax into lower energy QD level (in bigger size QDs). The competition of the carriers' thermal escape and recapture between the QD results in the redshifting of PL peak and the narrowing of the FWHM as the temperature increases. This explanation is totally consistent with the change in PL line shape with temperature shown in Fig. 1(a).

IV. CONCLUSIONS

In summary, we have reported electronic energy level and carrier dynamics of InAs/InGaAs DWELL structure. By combining PL and PLE spectra, we find direct evidence that the abnormal temperature dependent PL behavior of this structure is related to the carrier trapping in InGaAs QW. Referring to the electronic energy structure revealed by PLE spectrum, the temperature dependent integrated PL intensity is quantitatively described based on rate equation. With the discussion of the electronic energy structures and carrier dynamics, the temperature dependence of PL peak energy and FWHM are consistently explained.

- ¹H. Y. Liu, B. Xu, Y. Q. Wei, D. Ding, J. J. Qian, Q. Han, J. B. Liang, and Z. G. Wang, *Appl. Phys. Lett.* **79**, 2868 (2001).
- ²R. Ferreira and G. Bastard, *Appl. Phys. Lett.* **74**, 2818 (1999).
- ³H. Y. Liu, M. Hopkinson, C. N. Harrison, M. J. Steer, R. Frith, I. R. Sellers, D. J. Mowbray, and M. S. Skolnick, *J. Appl. Phys.* **93**, 2931 (2003).
- ⁴K. Mukai, N. Ohtsuka, and M. Sugawara, *Appl. Phys. Lett.* **70**, 2416 (1997).
- ⁵S. Sanguinetti, M. Padovani, M. Gurioli, E. Grilli, M. Guzzi, A. Vinattieri, M. Colocci, P. Frigeri, and S. Franchi, *Appl. Phys. Lett.* **77**, 1307 (2000).
- ⁶L. Seravalli, P. Frigeri, M. Minelli, P. Allegri, V. Avanzini, and S. Franchi, *Appl. Phys. Lett.* **87**, 063101 (2005).
- ⁷Y. T. Dai, J. C. Fan, Y. F. Chen, R. M. Lin, S. C. Lee, and H. H. Lin, *J. Appl. Phys.* **82**, 4489 (1997).
- ⁸E. C. Le Ru, J. Fack, and R. Murray, *Phys. Rev. B* **67**, 245318 (2003).
- ⁹S. Sanguinetti, M. Henini, M. Grassi Alessi, M. Capizzi, P. Frigeri, and S. Franchi, *Phys. Rev. B* **60**, 8276 (1999).
- ¹⁰B. Ilahi, L. Sfaxi, F. Hassen, H. Maaref, B. Salem, G. Guillot, A. Jbeli, and X. Marie, *Appl. Phys. A: Mater. Sci. Process.* **81**, 813 (2005).
- ¹¹A. Fiore, P. Borri, W. Langbein, J. M. Hvam, U. Oesterle, R. Houdré, R. P. Stanley, and M. Ilegems, *Appl. Phys. Lett.* **76**, 3430 (2000).
- ¹²T. V. Torchynska, J. L. C. Espinola, L. V. Borkovska, S. Ostapenko, M. Dybiec, O. Polupan, N. O. Korsunskaya, A. Stintz, P. G. Eliseev, and K. J. Malloy, *J. Appl. Phys.* **101**, 024323 (2007).
- ¹³B. Ilahi, L. Sfaxi, and H. Maaref, *J. Lumin.* **127**, 741 (2007).
- ¹⁴T. V. Torchynska, J. L. Casas Espinola, P. G. Eliseev, A. Stintz, K. J. Malloy, and R. Pena Sierra, *Phys. Status Solidi A* **195**, 209 (2003).
- ¹⁵D. P. Popescu, P. G. Eliseev, A. Stintz, and K. J. Malloy, *Semicond. Sci. Technol.* **19**, 33 (2004).
- ¹⁶T. V. Torchynska, J. L. Casas Espinola, E. Velázquez Losada, P. G. Eliseev, A. Stintz, K. J. Malloy, and R. Pena Sierra, *Surf. Sci.* **532–535**, 848 (2003).
- ¹⁷A. Lenz, H. Eisele, R. Timm, L. Ivanova, H. Y. Liu, M. Hopkinson, U. W. Pohl, and M. Dähne, *Physica E (Amsterdam)* **40**, 1988 (2008).
- ¹⁸H. Y. Liu, I. R. Sellers, T. J. Badcock, D. J. Mowbray, M. S. Skolnick, K. M. Groom, M. Gutierrez, M. Hopkinson, J. S. Ng, J. P. R. David, and R. Beanland, *Appl. Phys. Lett.* **85**, 704 (2004).
- ¹⁹H. Y. Liu, C. M. Tey, I. R. Sellers, T. J. Badcock, D. J. Mowbray, M. S. Skolnick, R. Beanland, M. Hopkinson, and A. G. Cullis, *J. Appl. Phys.* **98**, 083516 (2005).
- ²⁰H. D. Sun, M. D. Dawson, M. Othman, J. C. L. Yong, J. M. Rorison, P. Gilet, L. Grenouillet, and A. Million, *Appl. Phys. Lett.* **82**, 376 (2003).
- ²¹H. D. Sun, A. H. Clark, H. Y. Liu, M. Hopkinson, S. Calvez, M. D. Dawson, Y. N. Qiu, and J. M. Rorison, *Appl. Phys. Lett.* **85**, 4013 (2004).
- ²²G. Karczewski, S. Mackowski, M. Kutrowski, T. Wojtowicz, and J. Koszut, *Appl. Phys. Lett.* **74**, 3011 (1999).
- ²³R. Heitz, M. Veit, N. N. Ledentsov, A. Hoffmann, D. Bimberg, V. M.

- Ustinov, P. S. Kopev, and Z. I. Alferov, *Phys. Rev. B* **56**, 10435 (1997).
- ²⁴M. Bissiri, G. Baldassarri Höger von Högersthal, M. Capizzi, P. Frigeri, and S. Franchi, *Phys. Rev. B* **64**, 245337 (2001).
- ²⁵M. J. Steer, D. J. Mowbray, W. R. Tribe, M. S. Skolnick, M. D. Sturge, M. Hopkinson, A. G. Cullis, C. R. Whitehouse, and R. Murray, *Phys. Rev. B* **54**, 17738 (1996).
- ²⁶F. Adler, M. Geiger, A. Bauknecht, F. Scholz, H. Schweizer, M. H. Pilkuhn, B. Ohnesorge, and A. Forchel, *J. Appl. Phys.* **80**, 4019 (1996).
- ²⁷J. Johansen, S. Stobbe, I. S. Nikolaev, T. L. Hansen, P. T. Kristensen, J. M. Hvam, W. L. Vos, and P. Lodahl, *Phys. Rev. B* **77**, 073303 (2008).
- ²⁸A. Lévesque, N. Shtinkov, R. A. Masut, and P. Desjardins, *Phys. Rev. Lett.* **100**, 046101 (2008).
- ²⁹D. I. Lubyshev, P. P. González-Borrero, J. E. Marega, E. Petitprez, J. N. La Scala, and P. Basmaji, *Appl. Phys. Lett.* **68**, 205 (1996).
- ³⁰K. P. O'Donnell and X. Chen, *Appl. Phys. Lett.* **58**, 2924 (1991).
- ³¹M. Grundmann and D. Bimberg, *Phys. Rev. B* **55**, 9740 (1997).